Tethered Indenyl−Phosphine Complexes of Ruthenium(II) via Reductive Elimination of a Ruthenium(IV) Complex

Sin Yee Ng, Geok Kheng Tan, Lip Lin Koh, Weng Kee Leong,* and Lai Yoong Goh*

Department of Chemistry, National University of Singapore, Kent Ridge, Singapore 119260

Received March 9, 2007

The Ru(IV) phosphine complex [(η^3,η^3-$C_{10}H_{16}$)$RuCl_2$(κ^1P-**LH**)] (**2**) was synthesized from the reaction of [(η^3,η^3-$C_{10}H_{16}$)$RuCl_2$]$_2$ with [(C_9H_7)$(CH_2)_2PPh_2$] (**LH**). Treatment of **2** with acid led to halide labilization to give [(η^3,η^3-$C_{10}H_{16}$)$RuCl(CH_3CN)$(κ^1P-**LH**)]$^+$ [**2a**]$^+$. Reductive elimination of the bis(allyl) ligand in **2** was effected in the reaction of **2**, a two- or four-electron ligand (DD), Na_2CO_3, and KPF_6 in EtOH, resulting in the isolation of PF_6 salts of monocationic tethered indenyl Ru species, [(η^5,κ^1P-**L**)Ru(DD)] (**3**, DD = 1,5-cyclooctadiene (COD); **6**, DD = 2,2′-bipyridyl (bpy)), and neutral tethered indenyl Ru complexes (**4**, DD = (PPh_3)Cl; **5**, DD = (PPh_3)H). In addition to [**6**]PF_6, [(κ^1P-**LH**)Ru(bpy)$_2$Cl]PF_6, [**7**]PF_6, was an additional product in the bpy reaction, as was {[(κ^1P-**LH**)Ru(bpy)Cl]$_2$(μ-Cl)$_3$}PF_6, [**8**]-PF_6, when Na_2CO_3 was replaced by Li_2CO_3. In the presence of HCl, [**6**]$^+$ was found to convert to [**8**]$^+$, while [**8**]$^+$ was converted to [**7**]$^+$ with bpy and KPF_6. The reaction of **2** with acetylacetone (acacH) gave a high yield of an unusual complex, [(η^2,κ^1P-**LH**)Ru(acac)$_2$] (**9**), in which **LH** adopts a rare η^2,κ^1P-coordination mode. The new compounds were all spectroscopically characterized, with **2**, **2a**, **3**, **4**, and **9** also determined by single-crystal X-ray diffraction analyses.

Introduction

Compared to their parent Cp/Ind systems, organometallic complexes containing tethered cyclopentadienyl (η^5-C_5H_5, Cp) or indenyl (η^5-C_9H_7, Ind) ligands can exhibit quite different stability and reactivity characteristics,[1] including catalytic activity.[2] This has stimulated much work directed at the synthesis of ligands with variations on the Cp ring, the spacer, the heteroatom donor, and its substituent.[1e,3−6] Of keen interest is the combined effect of both metal-centered chirality and planar-chirality of Cp/Ind ligands on diastereoselectivity in reactions.[5,7,8] Planar-chirality can be induced by nonsymmetrical ring substitution, advantageously with a tethered ligand for asymmetric syntheses, or by an optically active substituent (e.g., neomenthyl or neoisomenthyl) in the Cp ring or the tether.[5b,c]

Scheme 1

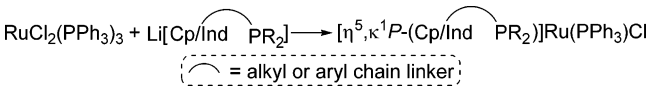

Since half-sandwich ruthenium complexes containing phosphine ligands are known to possess high catalytic activity for many reactions,[9] tethered Cp analogues have been of special interest. Indeed, the literature to date contains many examples of such phosphine-containing ruthenium(II) species, originating from the ruthenium precursor $RuCl_2(PR_3)_3$ (Scheme 1).[1b,3,5a,6] Recently, Takahashi reported the synthesis of tethered Cp−pyridine and −phosphine Ru(II) complexes containing acetonitrile co-ligands via displacement of a labile benzene ligand (Scheme 2a,c).[7] These are useful precursors to desired derivatives, wherein the labile acetonitrile ligands are substituted by bidentate ligands such as 2,2′-bipyridine and dithiocarbamate (Scheme 2b,d). Shortly after, Salzer and co-workers prepared analogous acetonitrile complexes from the reactions of the dimeric ruthenium(IV) complex [(η^3,η^3-$C_{10}H_{16}$)$RuCl_2$]$_2$ (**1**) in EtOH in the presence of CH_3CN and Li_2CO_3; the reaction occurred either via direct displacement of the 2,7-dimethyloctadienediyl ligand with a Cp-linked phosphine ligand (Scheme

* Corresponding author. E-mail: chmgohly@nus.edu.sg; chmlwk@nus.edu.sg. Fax: (+65) 6779 1691.

(1) (a) Becker, E.; Mereiter, K.; Puchberger, M.; Schmid, R.; Kirchner, K.; Doppiu, A.; Salzer, A. *Organometallics* **2003**, *22*, 3164. (b) Trost, B. M.; Vidal, B.; Thommen, M. *Chem.−Eur. J.* **1999**, *5*, 1055. (c) Foerstner, J.; Kakoschke, A.; Stellfeldt, D.; Butenschön, H.; Wartchow, R. *Organometallics* **1998**, *17*, 893. (d) Casey, C. P.; Czerwinske, C. J.; Fusie, K. A.; Hayashi, R. K. *J. Am. Chem. Soc.* **1997**, *119*, 3971. (e) Kataoka, Y.; Saito, Y.; Nagata, K.; Shibahara, A.; Tani, K. *Chem. Lett.* **1997**, 621. (f) Wang, S.; Li, H.-W.; Xie, Z. *Organometallics* **2004**, *23*, 2469. (g) Wang, S.; Li, H.-W.; Xie, Z. *Organometallics* **2004**, *23*, 3780.

(2) (a) Gareau, D.; Sui-Seng, C.; Groux, L. F.; Brisse, F.; Zargarian, D. *Organometallics* **2005**, *24*, 4003. (b) Groux, L. F.; Zargarian, D. *Organometallics* **2003**, *22*, 3124. (c) Groux, L. F.; Zargarian, D. *Organometallics* **2001**, *20*, 3811. (d) Buil, M. L.; Esteruelas, M. A.; López, A. M.; Concepción Mateo, A; Oñate, E. *Organometallics* **2007**, *26*, 554.

(3) (a) Siemeling, U. *Chem. Rev.*, **2000**, *100*, 1495. (b) Butenschön, H. *Chem. Rev.* **2000**, *100*, 1527. (c) Müller, C.; Vos, D.; Jutzi, P. *J. Organomet. Chem.* **2000**, *600*, 127. (d) Jutzi, P.; Redeker, T. *Eur. J. Inorg. Chem.* **1998**, 663. (e) Jutzi, P.; Siemeling, U. *J. Organomet. Chem.* **1995**, *500*, 175. (f) Jutzi, P.; Dahlaus, J. *Coord. Chem. Rev.* **1994**, *137*, 179.

(4) (a) Ciruelos, S.; Doppiu, A.; Englert, U.; Salzer, A. *J. Organomet. Chem.* **2002**, *663*, 183. (b) Doppiu, A.; Englert, U.; Peters, V.; Salzer, A. *Inorg. Chim. Acta* **2004**, *357*, 1773.

(5) (a) Kataoka, Y.; Saito, Y.; Nagata, K.; Shibahara, A.; Tani, K. *Chem. Lett.* **1995**, 833. (b) Kataoka, Y.; Iwato, Y.; Yamagata, T.; Tani, K. *Organometallics* **1999**, *18*, 5423. (c) Brookings, D. C.; Harrison, S. A.; Whitby, R. J.; Crombie, B.; Jones, R. V. H. *Organometallics* **2001**, *20*, 4574.

(6) Baker, R. W.; Luck, I. J.; Turner, P. *Inorg. Chem. Commun.* **2005**, *8*, 817.

(7) (a) Dodo, N.; Matsushima, Y.; Uno, M.; Onitsuka, K.; Takahashi, S. *J. Chem. Soc., Dalton Trans.* **2000**, 35. (b) Onitsuka, K.; Ajioka, Y.; Matsushima, Y.; Takahashi, S. *Organometallics* **2001**, *20*, 3274. (c) Matsushima, Y.; Onitsuka, K.; Takahashi, S. *Organometallics* **2004**, *23*, 3763. (d) Matsushima, Y.; Onitsuka, K.; Takahashi, S. *Organometallics* **2005**, *24*, 2747.

(8) (a) Kataoka, Y.; Shibahara, A.; Saito, Y.; Yamagata, T.; Tani, K. *Organometallics* **1998**, *17*, 4338. (b) Kataoka, Y.; Iwato, Y.; Shibahara, A.; Yamagata, T.; Tani, K. *Chem. Commun.* **2000**, 841.

(9) (a) Trost, B. M. *Acc. Chem. Res.* **2002**, *35*, 695, and references therein. (b) Trost, B. M.; Frederikson, M. U.; Rudd, M. T. *Angew. Chem., Int. Ed.* **2005**, *44*, 6630.

10.1021/om070225j CCC: $37.00
Publication on Web 06/01/2007

Scheme 2

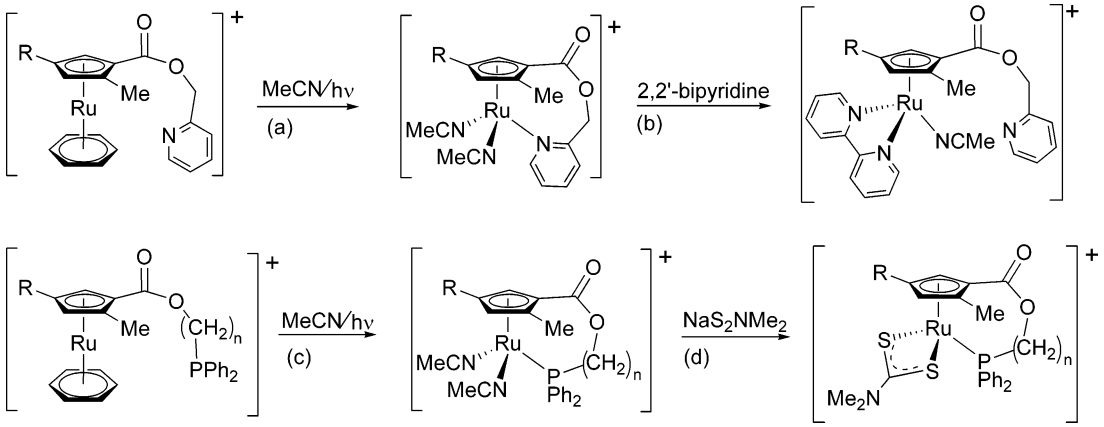

Scheme 3[10]

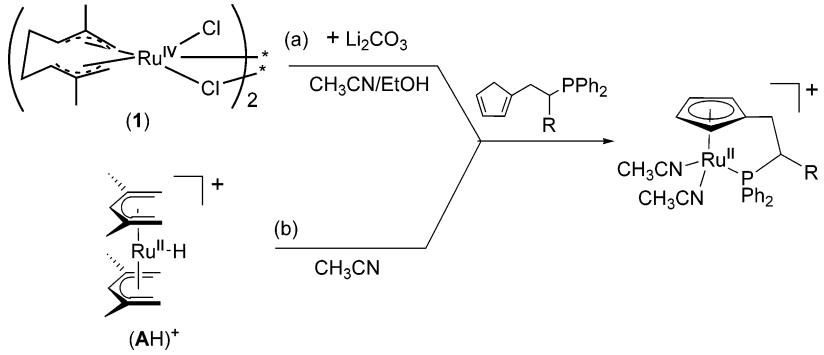

Scheme 4

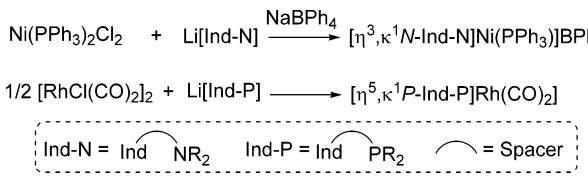

3a)[10a] or the reaction of the $[(\eta^5\text{-}C_7H_{11})_2HRu]^+$ (**A**H)$^+$ salt (obtained by protonation of **A**)[11] with the Cp-linked phosphine ligand in refluxing CH_3CN (Scheme 3(b)).[10b]

In comparison to Cp-tethered transition metal complexes, their indenyl analogues are scarce, with those of Ni,[2] Rh,[1e,5,8,12] and Ir[12c] being representative (Scheme 4). Enders had reported a stable complex of Cr(III) containing the Cp/Ind-N tether (N = 8-quinoline).[12d]

A recently reported Ru complex bears a tethered indenyl ligand containing an amino group through constrained coordination.[6] The relative scarcity of such tethered compounds is undoubtedly related to the lack of viable synthetic strategies. This study attempts to address the problem, and the results are described herein.

Results and Discussion

Synthesis. We tried route (b) in Scheme 3 using the Ind−phosphine ligand $IndHCH_2CH_2PPh_2$ (**LH**).[5b] The reaction proved unsuccessful, giving an inseparable complex mixture of products. We next reacted **1** with **LH** at ambient temperature for 4 h. However, unlike Salzer's reaction with $CpHCH_2CH(R)PPh_2$ or $CpHCH(R')CH_2PPh_2$,[10a] an Ind−P tethered complex was not formed, but instead only a phosphine derivative of **1**, viz., complex **2**, in high yield (Scheme 5). It appears probable that the presence of bulky substituents (R or R′) on the spacer carbons of the difunctional ligand predisposes the ligand toward tethering.

We therefore attempted to labilize the bis(allyl) ligand in **2** with an acid, the noncoordinating triflic acid, borrowing on the methodology of Werner and Stone in the use of carboxylic acids to labilize ruthenium−allyl bonds.[13] However, this reaction led only to the precipitation of the triflic salt of $[(\eta^3,\eta^3\text{-}C_{10}H_{16})RuCl(CH_3CN)(\kappa^1P\text{-}\mathbf{LH})]^+$, **[2a]**$^+$, a solvento derivative of **2** (Scheme 6). The intact bis(allyl) ligand indicates its inertness to protonation. It is likely that further chloride substitution in **[2a]**CF_3SO_3 had been prevented by its insolubility in the solvent medium. A double dehalogenation at Ru had been postulated to be essential for C_5H_6 (CpH) or C_9H_8 (IndH) to coordinate to the metal.[11]

The ^{1}H NMR spectra of **2** and **[2a]**$^+$ are consistent with the presence of **LH** and the $(\eta^3,\eta^3\text{-}C_{10}H_{16})$ ligand. The ^{31}P NMR spectrum of **2** shows a signal at δ 18.9, a typical chemical shift for a coordinated phosphine ligand. The ^{31}P signal of **[2a]**$^+$ is found in a lower field at δ 22.2.

The ORTEP diagrams of **2** and **[2a]**$^+$ are shown in Figure 1 and 2, respectively, and selected bond lengths and bond angles are given in Table 1. The X-ray structure of **2** shows that there are two independent molecules and one ether molecule in the

(10) (a) Doppiu, A.; Englert, U.; Salzer, A. *Inorg. Chim. Acta* **2003**, *350*, 435. (b) Doppiu, A.; Salzer, A. *Eur. J. Inorg. Chem.* **2004**, 2244.

(11) Bauer, A.; Englert, U.; Geyser, S.; Podewils, F.; Salzer, A. *Organometallics* **2000**, *19*, 5471.

(12) (a) Kataoka, Y.; Shibahara, A.; Yamagata, T.; Tani, K. *Organometallics* **2001**, *20*, 2431. (b) Kataoka, Y.; Nakagawa, Y.; Shibahara, A.; Yamagata, T.; Mashima, K.; Tani, K. *Organometallics* **2004**, *23*, 2095. (c) Kataoka, Y.; Shimada, K.; Goi, T.; Yamagata, T.; Mashima, K.; Tani, K. *Inorg. Chim. Acta* **2004**, *357*, 2965. (d) Enders, M.; Fernández, P.; Ludwig, Pritzkow, H. *Organometallics* **2001**, *20*, 5005.

(13) See for instance: (a) Werner, H.; Fries, G.; Woberndörfer, B. *J. Organomet. Chem.* **2000**, *607*, 182. (b) Dossett, S. J.; Li, S.; Stone, F. G. A. *J. Chem. Soc., Dalton Trans.* **1993**, 1585.

Scheme 5

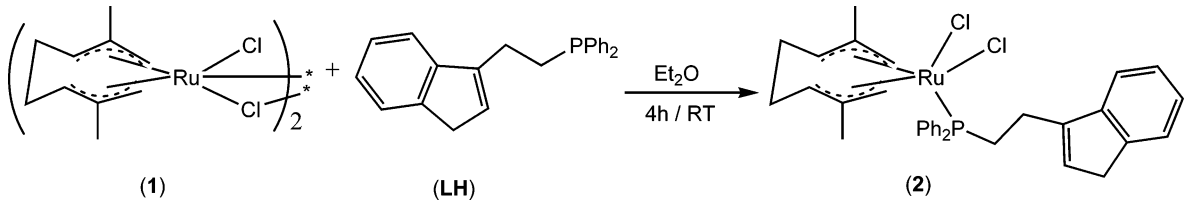

Scheme 6

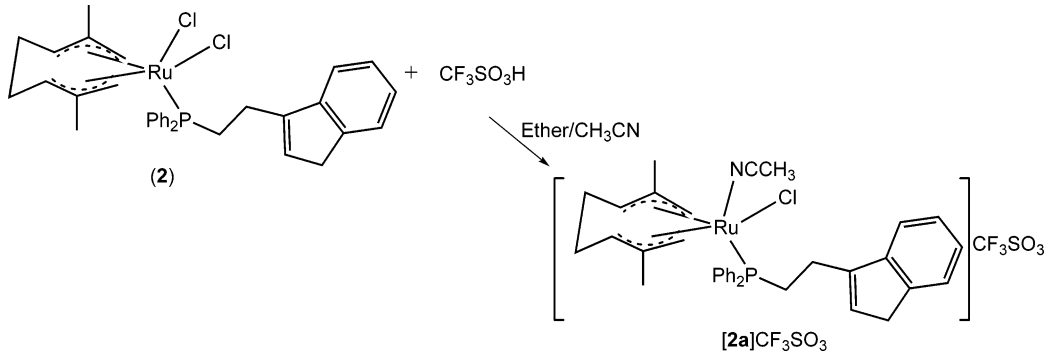

Table 1. Selected Bond Lengths and Angles for 2 and [2a]$^{+}$ [a]

bond length (Å)	**2**	[**2a**]$^{+}$	bond angles (deg)	**2**	[**2a**]$^{+}$
Ru(1)−P(1)	2.4144(11)	2.4050(16)	D(1)−Ru(1)−D(2)	130.51	130.87
Ru(1)−Cl(1)	2.4179(11)	2.4094(18)	D(1)−Ru(1)−Cl(1)	92.54	94.08
Ru(1)−X	X = Cl(2), 2.4331(11)	X = N(1), 2.031(6)	D(1)−Ru(1)−X	X = Cl(2), 88.23	X = N(1), 88.03
Ru(1)−C(12)	2.216(4)	2.274(6)	D(1)−Ru(1)−P(1)	114.63	115.08
Ru(1)−C(13)	2.295(4)	2.299(6)	D(2)−Ru(1)−Cl(1)	88.02	89.77
Ru(1)−C(14)	2.280(4)	2.252(6)	D(2)−Ru(1)−X	X = Cl(2), 92.01	X = N(1), 91.72
Ru(1)−C(17)	2.277(4)	2.201(6)	D(2)−Ru(1)−P(1)	114.85	114.04
Ru(1)−C(18)	2.275(4)	2.273(7)	Cl(1)−Ru(1)−X	X = Cl(2), 174.00(4)	X = N(1), 175.65(15)
Ru(1)−C(19)	2.231(4)	2.278(6)	Cl(1)−Ru(1)−P(1)	89.71(4)	84.42(6)
Ru(1)−D(1)	2.011	2.025	P(1)−Ru(1)−X	X = Cl(2), 84.56(4)	X = N(1), 91.24(15)
Ru(1)−D(2)	2.006	2.003	Ru(1)−P(1)−C(1)	115.82(15)	114.6(2)
C(3)−C(4)	1.326(7)	1.317(11)	C(2)−C(1)−P(1)	115.2(3)	115.3(4)
C(3)−C(11)	1.469(6)	1.501(12)			
C(4)−C(5)	1.490(7)	1.567(16)			
C(5)−C(6)	1.505(8)	1.473(18)			

[a] D(1) and D(2) are the centroids of atoms C(12), C(13), C(14) and C(17), C(18), C(19), respectively.

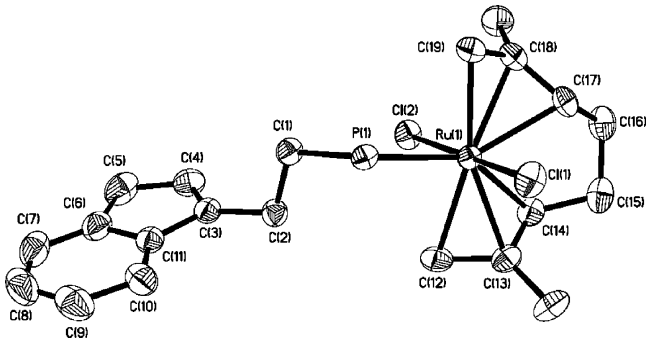

Figure 1. ORTEP diagram of **2** (50% probability thermal ellipsoids, hydrogen atoms and Ph rings have been omitted for clarity).

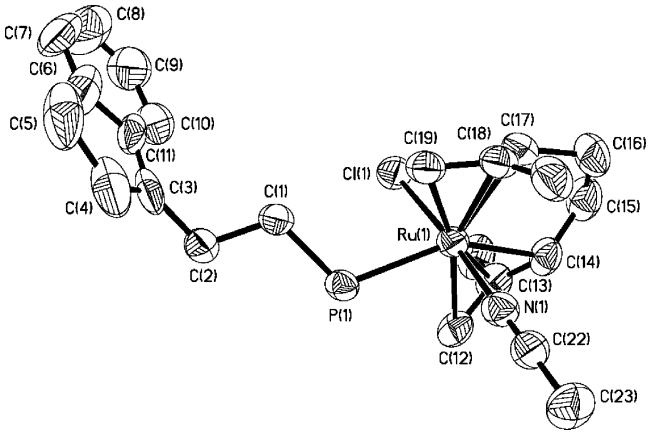

Figure 2. ORTEP diagram of **2a** cation (50% probability thermal ellipsoids, hydrogen atoms and Ph rings have been omitted for clarity).

asymmetric unit, while the asymmetric unit of [**2a**]CF_3SO_3 contains one molecule of [**2a**]$^{+}$ and a disordered $CF_3SO_3^{-}$ anion. The molecular structures of **2** and [**2a**]$^{+}$ are very similar to those of other reported bis(allyl) Ru(IV) complexes, e.g., $RuCl_2(\eta^3,\eta^3\text{-}C_{10}H_{16})P$ (P = $Ph_2PNHC_6H_4PPh_2$,[14] $Ph_2PNHNHpy$[15]) and $RuCl(\eta^3,\eta^3\text{-}C_{10}H_{16})(CH_3CN)_2$.[16] The coordination geometries around the Ru center in both **2** and [**2a**]$^{+}$ are distorted trigonal pyramidal, with bis(allyl) and the κ^1P-**LH** ligand occupying the equatorial positions. It was noticed that the phosphorus atom is

(14) Aucott, S. M.; Slawin, A. M. Z.; Woolins, J. D. *J. Organomet. Chem.* **1999**, *582*, 83.

(15) Slawin, A. M. Z.; Wheatley, J.; Wheatley, M. V.; Woolins, J. D. *Polyhedron* **2003**, *22*, 1397.

(16) Cox, D. N.; Small, R. W. H.; Roulet, R. *J. Chem. Soc., Dalton Trans.* **1991**, 2013.

Scheme 7

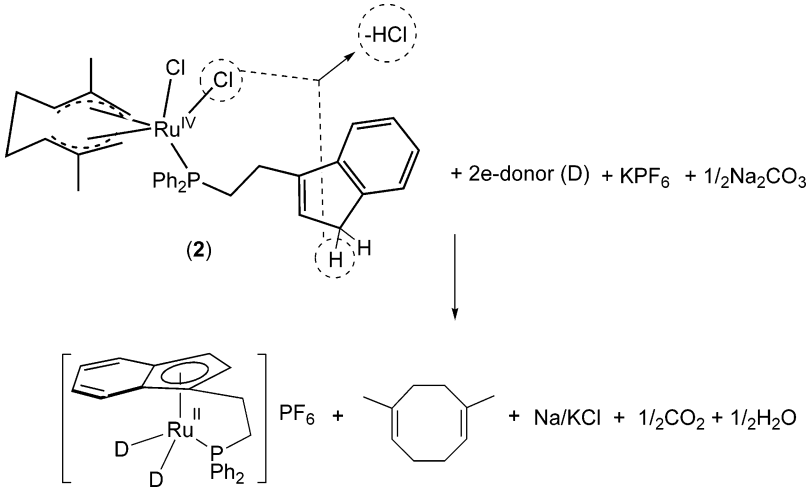

Scheme 8

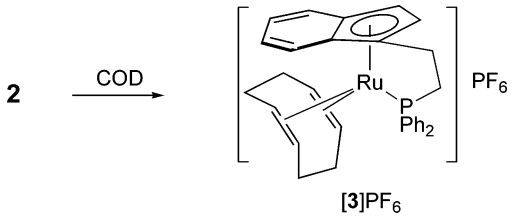

almost equidistant from D1 and D2, the centroids of atoms C(12), C(13), C(14) and C(17), C(18), C(19), respectively, in **2**, while the phosphorus atom is closer to D2 than to D1 in [**2a**]$^+$. The lack of symmetry in the bis(allyl) ligand in [**2a**]$^+$ is reflected in the ^{1}H NMR spectroscopic data.

Subsequent to the above negative synthetic outcomes, we attempted reductive elimination of the bis(allyl) ligand in the presence of two- or four-electron donor ligands and a base or a halogen abstractor (Scheme 7). Indeed, we found that the reaction of **2** with 1,5-cyclooctadiene (COD) in the presence of $AgPF_6$ in EtOH solution proceeded at room temperature to give [(η^5,κ^1*P*-**L**)Ru(COD)]PF_6, [**3**]PF_6, in high yield. The same result was obtained by refluxing **2** with COD in EtOH, in the presence of finely ground Na_2CO_3 and KPF_6 (Scheme 8). In fact this latter set of reagents has proven more useful, as it is compatible with different classes of incoming ligands, e.g., phosphine donors such as PPh_3, nitrogen donors such as 2,2′-bipyridyl, and oxygen donors such as acac, in which cases the Ag^+ ion interferes. Additionally it was observed that the particle size of the base was a crucial factor on the yield, consistent with the heterogeneous nature of the reaction.[17]

The ^{1}H NMR signals for the COD ligand in [**3**]PF_6 appear in the range δ 0.66−2.20 for CH_2 and δ 3.52−4.04 for CH, while the protons of the ethylene side arm resonate as two multiplets in the range δ 2.32−2.89. The ^{31}P signal appears at δ 67.7, which is within the low-field range [δ 52−88] reported for the tethered complex [(η^5,κ^1*P*-Cp$(CH_2)_2PPh_2$)Ru$(CH_3CN)_2$]PF_6.[10b]

The molecular structure of [**3**]$^+$ showing the η^5,κ^1*P*-coordination mode of **L** is illustrated in Figure 3. There is no significant difference between its bond parameters and those of its Ind analogue, [(η^5-Ind)Ru(COD)(py)]BF_4.[18] The slip-fold parameters for [**3**]PF_6 are (i) slip distortion (Δ) = 0.122 (7) Å, (ii) hinge angle (HA) = 5.1°, and (iii) fold angle (FA) = 8.3°, indicating that the indenyl ligand is coordinated to the Ru center via a distorted η^5-mode.[19]

The reactions of **2** with N-, P-, and O-donor ligands in the presence of 1 equiv of Na_2CO_3 in EtOH have been studied. The reaction with PPh_3 gave a mixture of [(η^5,κ^1*P*-**L**)Ru(PPh_3)-Cl] (**4**) and [(η^5,κ^1*P*-**L**)Ru(PPh_3)H] (**5**) (isolated in ca. 4:1 relative yield). Both **4** and **5** were obtained in only one diastereomeric form each. The formation of **5** was hindered by reducing the amount of Na_2CO_3; at zero or 0.5 mol equiv to **2**, none of **5** was formed, while the yield of **4** increased to 82%. A plausible formation pathway is proposed in Scheme 9, in which Na_2CO_3 is required for the functions of chloride and proton abstraction (routes (a) and (b), respectively). A separate reaction showed that complex **5** can be obtained in high yield

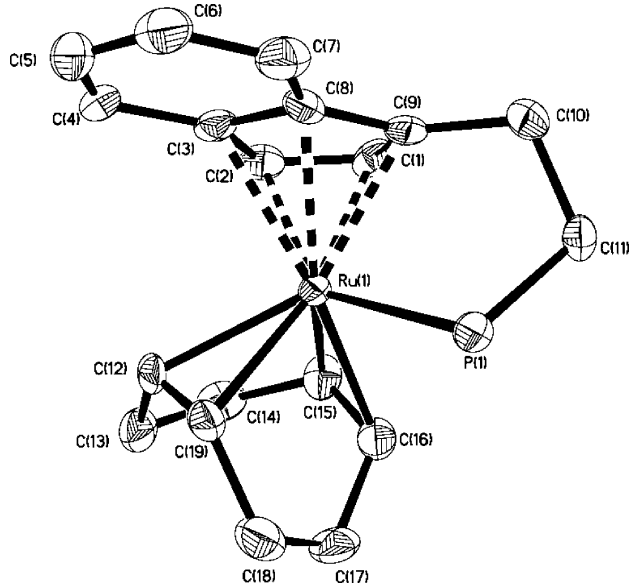

Figure 3. ORTEP diagram of [**3**]$^+$ (50% probability thermal ellipsoids, hydrogen atoms and Ph rings have been omitted for clarity). Selected bond lengths (Å) and angles (deg). Ru(1)−P(1) = 2.3995(18); Ru(1)−C(12) = 2.223(6); Ru(1)−C(19) = 2.214-(6); Ru(1)−C(15) = 2.212(7); Ru(1)−C(16) = 2.221(7); Ru(1)−C* = 1.911; C*−Ru(1)−C(12) = 115.62; C*−Ru(1)−C(15) = 112.24; C*−Ru(1)−C(16) = 141.12; C*−Ru(1)−C(19) = 137.55; C*−Ru(1)−P(1) = 107.88; C(15)−Ru(1)−C(16) = 37.2(2); C(12)−Ru(1)−C(19) = 36.4(3); Ru(1)−P(1)−C(11) = 100.0(2) (C* = centroid of the five-membered ring, comprising C(1), C(2), C(3), C(8), and C(9)).

(17) Salzer, A.; Bauer, A.; Geyser, S.; Podewils, F. *Inorg. Synth.* **2004**, *34*, 59.

(18) Alvarez, P.; Gimeno, J.; Lastra, E.; García-Granda, S.; Van der Maelen, J. F.; Bassetti, M. *Organometallics* **2001**, *20*, 3762.

Scheme 9

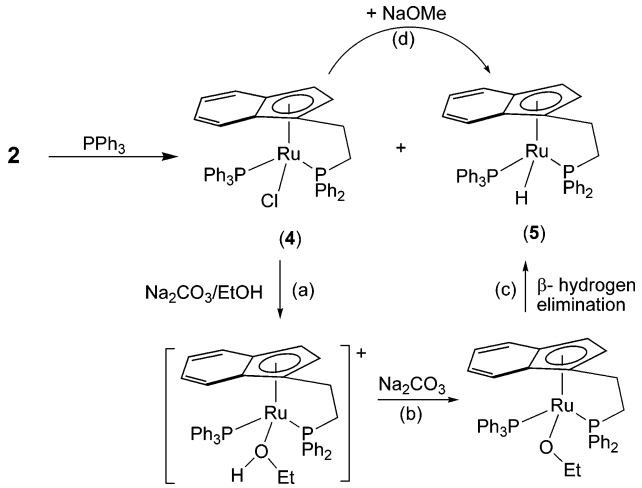

by refluxing **4** with NaOMe (pathway (d)). Hydride formation in thiolate substitution reactions of (Ind)Ru(dppf)Cl had been shown to be effected by the generation of methoxide via an equilibrium between thiolate RS^- and MeOH;[20a] indeed, the synthesis of (Cp/Ind)Ru hydrides from halide precursors via methoxide intermediates is a standard methodology.[20b−d]

The ^{1}H NMR spectrum of **4** shows five sets of multiplets in the range δ 1.42−3.22, assigned to the protons of the ethylene side arm of the **L** ligand. On the basis of a 2D-COSY NMR measurement, the two singlets at δ 2.26 and 4.87 are assigned to the protons on the five-membered ring of **L**. The upfield chemical shift (δ 2.26) of the protons on the Cp ring of the indenyl ligand had been observed at δ 3.56 in the tethered indenyl Ni complex, [(η^5-Ind$(CH_2)_2$(CH═CH_2))Ni(PPh_3)Cl].[2a,21] This is consistent with the X-ray structural analysis (see Figure 4), which shows the indenyl proton, H12, pointing directly toward the center of the phenyl ring and hence subjected to shielding by the ring current of the phenyl ring of PPh_3.

The ^{1}H NMR spectrum of **5** shows a characteristic hydride signal at δ −13.9 as a doublet of a doublet, consistent with coupling to two P atoms of the phosphane ligands. The protons of the indenyl Cp ring resonate in the "normal" range at δ 4.78 and 5.48. This observation implies that the orientation of the Cp ring in **5** is different from that in **4**, but unfortunately X-ray crystal structural data could not be obtained.

The reaction of **2** with 1 molar equiv of 2,2′-bipyridyl (bpy) in the presence of Na_2CO_3 and KPF_6 led to the formation of [(η^5,κ^1*P*-**L**)Ru(bpy)]PF_6 ([**6**]PF_6) and [(κ^1*P*-**LH**)Ru(bpy)$_2$Cl]PF_6 ([**7**]PF_6) in ca. 2:1 molar ratio (Scheme 10(i)). An inverse relative yield (i.e., 1:2) of species [**6**]PF_6 and [**7**]PF_6, was obtained when Na_2CO_3 was replaced by Li_2CO_3; in addition, a new product, {[(κ^1*P*-**LH**)Ru(bpy)Cl]$_2$(μ-Cl)$_3$}PF_6, [**8**]PF_6, was formed (Scheme 10(ii)). The glaring difference in the composition of these complexes is the presence of chloride in [**7**]PF_6 and [**8**]PF_6 and its absence in [**6**]PF_6. A very plausible rationale for the difference in the two situations therefore lies in the greater availabilty of chloride ions in the Li_2CO_3 case, arising from the higher solubility of LiCl versus NaCl in EtOH. This also explains the additional formation of species [**8**]PF_6 with even higher Cl^- content. The supply of Cl^- from HCl was found to convert complex [**6**]PF_6 completely to complex [**8**]PF_6, (Scheme 10(iii)), but this conversion could not be effected with NaCl. [**6**]PF_6 with HCl converted to a mixture of complexes [**7**]PF_6 and [**8**]PF_6 in the added presence of 1.5 molar equiv of bpy (Scheme 10(iv)). In addition it was found that in the presence of 1 molar equiv of bpy and KPF_6, [**8**]PF_6 was transformed to [**7**]PF_6 (Scheme 10(v)). It was also observed that the reaction of **2** with a 4-fold excess of bpy resulted in total displacement of all the ligands, giving [Ru(bpy)$_3$]$(PF_6)_2$ as the sole product. In context, we note that Salzer and co-workers had observed a marked effect of the carbonate bases of group 1 metals (Li > Na > K) on the yield of the sandwich bis(dienyl) complex [(η^5-$C_7H_{11})_2$Ru] (**A**) from the reaction of **1** with dimethylpentadiene; this had been ascribed to solubility differences of the solid bases in the reaction medium.[11]

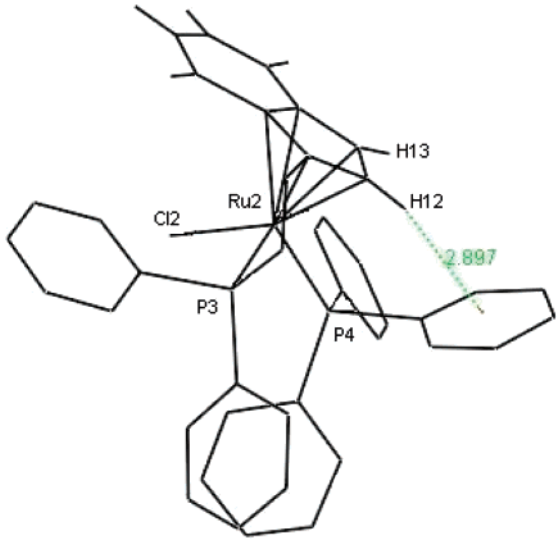

Figure 4. Molecular structure of **4**.

The proposed formulations of species [**6**]PF_6, [**7**]PF_6, and [**8**]-PF_6 were based on microanalytical and spectroscopic evidence. The coordination mode of **L** and **LH** in the cationic complexes [**6**]PF_6, [**7**]PF_6, and [**8**]PF_6 can be determined by their resonances in the ^{1}H NMR spectra. The protons of the Cp ring of (η^5,κ^1*P*-**L**)in [**6**]PF_6 appear at δ 5.21 and 5.53, indicating the aromaticity at the Cp ring, while the protons of the five-membered ring of (κ^1*P*-**LH**) in species [**7**]PF_6 and [**8**]PF_6 are found at δ 6.10 (for the "-ene" proton) and δ 3.23 (for the sp^3-protons). The ^{31}P NMR spectrum also gave significant insight into the coordination mode of the ligand as the ^{31}P signal of (η^5,κ^1*P*-**L**) in [**6**]-PF_6 resonates at δ 61.7, which is at lower field than the ^{31}P signal of (κ^1*P*-**LH**) in [**7**]PF_6 (δ 39.5) and [**8**]PF_6 (δ 54.5). Their mass spectra showed their mother ion peaks. While the isotopic distribution patterns of the signals showed that [**6**]PF_6 and [**7**]-PF_6 are mononuclear species, that of [**8**]PF_6 indicated a dinuclear species.

The reaction of **2** with 1 molar equiv of acetyl acetone in the presence of 2 molar equiv of Na_2CO_3 gave a multicomponent product mixture from which complex [(η^2,κ^1*P*-**LH**)Ru(acac)$_2$] (**9**) was isolated in 38% yield (Scheme 11). A repeat experiment

(19) For indenyl complexes containing undistorted η^5 rings: Δ = 0.03 Å; HA = 2.5 °; FA = 4.4°; for those containing distorted η^5 rings: Δ = 0.11−0.42 Å; HA = 7−14°; FA = 6−13°; and for those wherein the five-membered ring is η^3-coordinated: Δ = 0.8 Å; FA = 28°. See: Kakkar, A. K.; Taylor, N. J.; Marder, T. B.; Shen, J. K.; Hallinan, N.; Basolo, F. *Inorg. Chim. Acta* **1992**, *198*−*200*, 219.

(20) (a) Ng, S. Y.; Leong, W. K.; Goh, L. Y.; Webster, R. D. *Eur. J. Inorg. Chem.* **2007**, 463. (b) Bruce, M. I.; Humphrey, M. G.; Swincer, A. G.; Wallis, R. C. *Aust. J. Chem.* **1984**, *37*, 1747. (c) Bassetti, M.; Casellato, P.; Gamasa, M. P.; Gimeno, J.; González-Bernardo, C.; Martín-Vaca, B. *Organometallics* **1997**, *16*, 5470. (d) Gamasa, M. P.; Gimeno, J.; González-Bernardo, C.; Martín-Vaca, B.; Borge, J.; Garcia-Granda, S. *Inorg. Chim. Acta* **2003**, *347*, 181.

(21) Zargarian, D. *Coord. Chem. Rev.* **2002**, *233*−*234*, 157.

Scheme 10

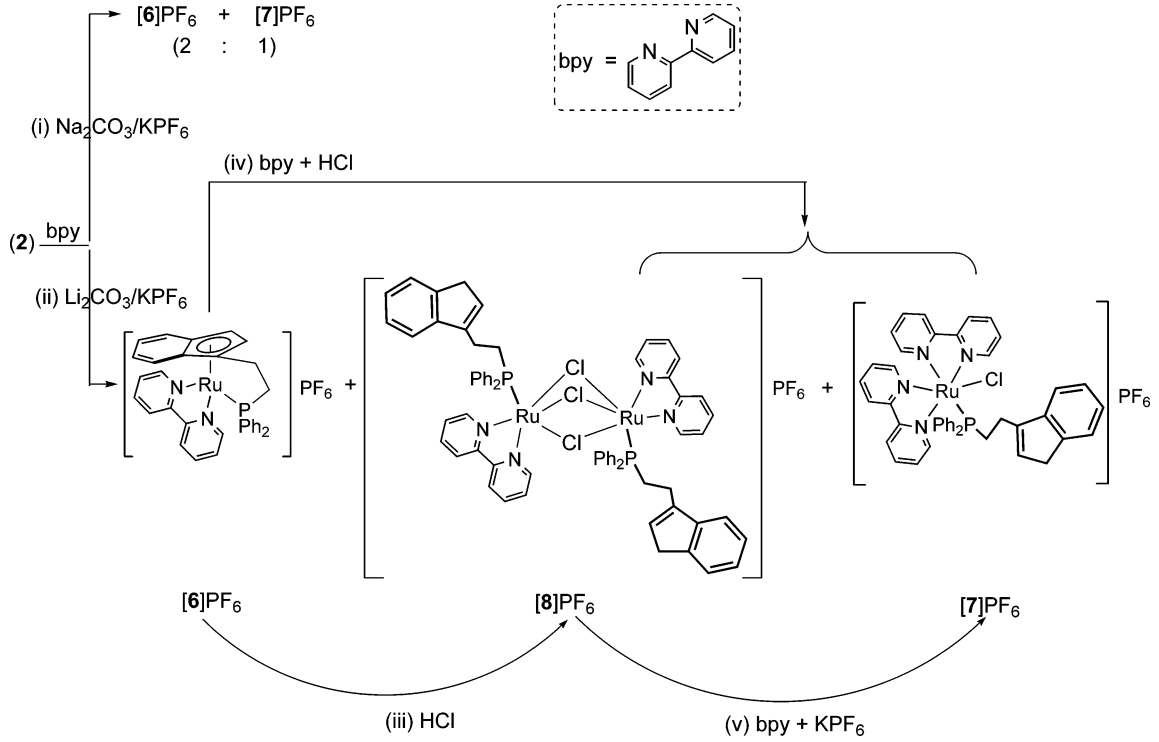

Scheme 11

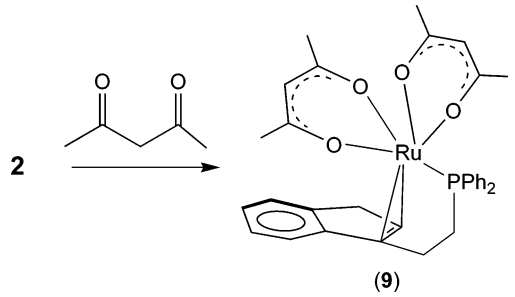

using the correct stoichiometric amount of acetyl acetone to **2** in the presence of an appropriate molar equivalent of Na_2CO_3 gave an increased yield of **9** (78%) from a cleaner product mixture. In complex **9**, the Ru(II) center is coordinated to two chelating acac ligands and an **LH** ligand in an uncommon η^2,κ^1P-coordination mode.

Complex **9** was characterized by single-crystal X-ray diffraction analysis. The asymmetric unit contains two independent tilted molecules, the structures of which are very similar. This is shown in Figure 5, with selected bond parameters for one of the molecules. The Ru(II) center adopts a pseudo-octahedral geometry, with coordination to the four O atoms of two acac ligands, a P donor atom, which with O(4) occupies equatorial positions, and an "ene" C(1)−C(9) moiety taking up the sixth position, which is axial and trans to O(3). The (η^2,κ^1P-**LH**) coordination mode to Ru is rare and had been observed before only in the (η^2,κ^1N-Ind-quinolyl) tethered complexes of Rh(I) and Mo(0).[22] Ethene complexes of acac-containing Ru(II) are known, e.g., *cis*-Ru(acac)$_2$(η^2-C_2H_4)$_2$ (**B**) and derivatives thereof.[23] The bonding mode in **9** bears a slight resemblance to that found in [(η^5-Ind)Ru(κ^3(*P,C,C*)-$Ph_2P(CH_2CH{=}CH_2)$)(PPh_3)]$^+$ (**C**), in which Ru is coordinated to P and the terminal alkene of a phosphino ligand;[24] the phosphine is homoallylic in **9** but allylic in the latter. The C(1)−C(9) bond length (1.392(4) Å, clearly of double-bond character, is close to that in **C** (1.391(8) Å)[24] but longer than those in coordinated unsubstituted ethenes in **B** and its monoethene derivatives (range 1.35(1)−1.37(3) Å).[23] The Ru(1)−P(1) distance is substantially shorter ($\Delta \approx 0.06$−0.09 Å) than the analogous distance in **C**.[24] The Ru(1)−C(1) distance is comparable to the equivalent distances in **B**;[23] however the Ru(1)−C(9) bond is significantly longer (Δ =

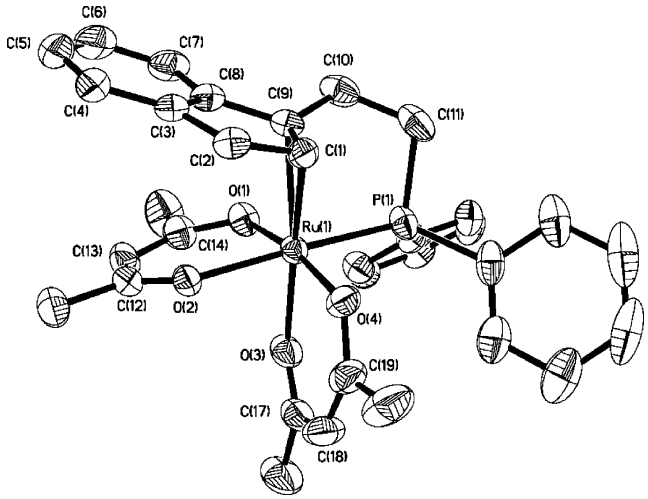

Figure 5. ORTEP diagram of **9** (50% probability thermal ellipsoids, hydrogen atoms omitted) and selected bond lengths (Å) and angles (deg): Ru(1)−O(1) = 2.0563(19); Ru(1)−O(2) = 2.1067(18); Ru(1)−O(3) = 2.069(2); Ru(1)−O(4) = 2.0670(19); Ru(1)−P(1) = 2.2495(8); Ru(1)−C(1) = 2.186(3); Ru(1)−C(9) = 2.252(3); C(1)−C(9) = 1.392(4); C(1)−C(2) = 1.513(4); O(1)−Ru(1)−O(2) = 90.23(8); O(3)−Ru(1)−O(4) = 89.53(9); C(1)−Ru(1)−C(9) = 36.53(10); C(1)−C(9)−C(8) = 107.3(2); C(1)−C(9)−C(10) = 128.2(3); C(8)−C(9)−C(10) = 119.4(2); C(9)−C(1)−C(2) = 110.7(2); C(9)−C(1)−Ru(1) = 74.32(16); C(2)−C(1)−Ru(1) = 113.82(19).

(22) Enders, M.; Fernández, P.; Kaschke, M.; Kohl, G.; Ludwig, G.; Pritzkow, H.; Rudolph, R. *J. Organomet. Chem.* **2002**, *641*, 81.

(23) Bennett, M. A.; Byrnes, M. J.; Willis, A. C. *Organometallics* **2003**, *22*, 1018.

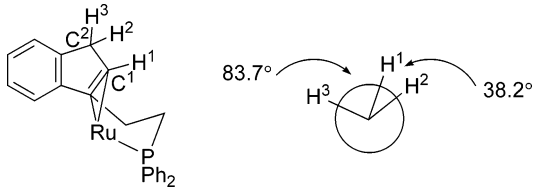

Figure 6. Hydrogen atoms-labelling of the indenyl 5-membered ring of **9**.

0.066 Å), understandably an effect of the asymmetry of the ethene moiety with higher steric constraint at bridgehead-like C(9). In contrast, complex **C** shows only a small difference in the Ru−C bonds of the metal center to the ethene moiety. While the Ru(1)−O distances in **9** (range 2.0563(19)−2.1067(18) Å) are similar to those in Bennett's Ru(acac) complexes, the Ru-(1)−O(2) bond is substantially longer ($\Delta \approx 0.04-0.05$ Å), rationalized as a consequence of the trans effect of the P donor atom.

The spectroscopic data of **9**, obtained from a proton NMR scan and a 2D-COSY experiment, are consistent with the structure. Thus, the proton spectrum shows the four chemically inequivalent Me groups of the two acac ligands at δ 1.34−1.80 and the allylic protons at δ 4.29 and 4.96. The protons on C10 and C11, the ethylene side arm, appear as four sets of multiplets in the range δ 2.32−2.89. Referring to the atom-labeling code shown in Figure 6, the "ene" proton (H^1 on C1) of the five-membered ring of Ind appears as a doublet at δ 5.15 with $^3J_{HH} = 3.7$ Hz (coupling with H^2), while the sp^3-protons H^2 on C2 appears as a doublet of a doublet at δ 3.39 ($^3J_{HH} = 3.7$ Hz and $^2J_{HH} = 20$ Hz) and H^3 appears as a doublet at δ 3.61 ($^2J_{HH} = 20$ Hz; coupling with H^2). The correlation of each signal was established using 2D-COSY NMR spectroscopy. There was no coupling observed between H^3 and H^1. This observation was further supported by the X-ray structure, which shows that H^1 and H^3 are almost orthogonal (83.7°) and therefore will have minimal transmission of nuclear spin information, resulting in no coupling, according to Karplus rule.[25] The angle between H^2 and H^3 is 109.2°, with a geminal coupling constant of 20 Hz, which is slightly larger than the $^2J_{HH}$ of a typical sp^3 protons on a C_6 ring with angle between the protons of ~109°.[25]

The formation of the Ru(II) complex **9** had involved multiple processes, viz., chloride abstraction from **2** by Na^+ ions, followed by coordination of two $acac^-$ ligands with displacement of the bis(allyl) ligand. This so-formed 16-electron "intermediate" would not be able to accept a η^5-indenyl ligand, unless one of the acac ligands can be displaced. That this had not occurred is consistent with the relative bond strength of the $acac^-$ versus η^5-ind ligands. The metal center of the "intermediate" therefore achieves its 18-electron configuration by coordinating to the "-ene" moiety of the **LH** ligand, giving rise to a (η^2,κ^1P-) bonding mode at Ru(II).

Attempts to synthesize the (η^5,κ^1P-**L**)Ru(II) complex with labile CH_3CN ligands were in vain, as refluxing **2** in a solvent mixture of EtOH/CH_3CN (1:1), Na_2CO_3, and KPF_6 led only to an inseparable complex mixture, indicating the need of strong donor ligands to stabilize (η^5,κ^1P-**L**)Ru(II) complexes.

Conclusion

A synthetic route has been developed for the transformation of bis(allyl)Ru(IV) precursor **2** to tethered [(η^5,κ^1P-**L**)Ru(II)] complexes containing COD, PPh_3, and 2,2′-bipyridyl ligands. While **L** adopts the expected η^5,κ^1P-coordination mode in complexes [**3**]$^+$, **4**, **5**, and [**6**]$^+$, it was also found to coordinate either via a κ^1P-**LH**, as in [**7**]$^+$ and [**8**]$^+$, or via a rare η^2,κ^1P-**LH** coordination mode, as found in **9**. The reaction methodology used here could be a potentially convenient route to more examples of tethered indenyl Ru derivatives.

Experimental Section

General Procedures. All reactions were carried out using conventional Schlenk techniques under an inert atmosphere of nitrogen or under argon in an M. Braun Labmaster 130 inert gas system.

NMR spectra were measured on a Bruker 300 FT NMR spectrometer, while that of **9** and the 2D-COSY spectra of **4** and **9** were recorded on a Bruker 500 FT NMR spectrometer; for ^1H and ^{31}P spectra, chemical shifts were referenced to residual solvent in the deuterosolvents C_6D_6 and $(CD_3)_2CO$. IR spectra in KBr pellets were measured in the range 4000−400 cm^{-1}, using a BioRad FTS-165 FTIR instrument. Mass spectra were run on a Finnigan Mat 95XL-T (FAB) or a Finnigan-MAT LCQ (ESI) spectrometer. Elemental analyses were performed by the microanalytical laboratory in-house.

$[(C_{10}H_{16})RuCl_2]_2$ (**1**)[17] and $IndH(CH_2)_2PPh_2$ (**LH**)[5b] were prepared by published methods. All other chemicals were obtained commercially and used as supplied. All solvents were dried over sodium/benzophenone and distilled before use. Celite (Fluka AG), silica gel (Merck Kieselgel 60, 230-400 Mesh), and neutral alumina (acitivity III) were dried at 140 °C overnight before chromatographic use. **Synthesis of [(η^3,η^3-$C_{10}H_{16}$)$RuCl_2$(κ^1P-LH)] (2). 1** (100 mg, 0.16 mmol) was added into an ether solution of **LH** (106 mg, 0.32 mmol, 10 mL), and the suspension was stirred for 4 h, whereupon the color of the suspension changed slowly from purplish red to yellow. Yellow solids of **2** were filtered (93 mg, 45% yield). The filtrate was concentrated to ca. 1 mL, and hexane (ca. 5 mL) was added. A second crop of yellow microcrystals of **2** were obtained after 1 day at −30 °C (73 mg, 35% yield). Single crystals of X-ray diffraction quality were obtained from a solution of **2** in CH_2Cl_2 layered with hexane after 2 days at −30 °C.

Data for 2. ^1H NMR (CD_3CN): δ 2.15 (s, 6 H, Me), 2.24−2.38 (m, 2 H, $IndH(CH_2)_2PPh_2$), 2.50−2.60 (m, 2 H, $IndH(CH_2)_2PPh_2$), 2.63−2.68 (m, 2 H, H^d and H^f), 3.12−3.14 (d-like, 2 H, H^b and H^j), 3.29 (s, 2 H, H^{2-3}), 3.39−3.45 (m, 2 H, H^e and H^g), 4.24−4.28 (d-like, 2 H, H^a and H^i), 5.12 (br s, 2 H, H^c and H^h), 6.26 (s, 1 H, H^1), 7.10−7.21, 7.42−7.49, 7.72−7.78, and 7.86−7.92 (each m, total 14 H, Ph and H^{4-7}). $^{31}P\{^1H\}$ NMR (CD_3CN): δ 18.9 (s, $IndH(CH_2)_2PPh_2$). FAB^+-MS: *m/z* 636 $[M]^+$, 601 $[M - Cl]^+$, 565 $[M - 2Cl]^+$, 464 $[M - C_{10}H_{16} - Cl]^+$, 429 $[M - C_{10}H_{16} - 2Cl]^+$. Anal. Calc (Found) for $C_{33}H_{37}Cl_2PRu$: C, 62.3 (62.1); H, 5.9 (6.0).

Synthesis of [((η^3,η^3-$C_{10}H_{16}$)$RuCl(CH_3CN)$(κ^1P-LH)](CF_3SO_3) (2a·CF_3SO_3). CF_3SO_3H (9 μL, 0.10 mmol) was slowly injected into a stirred solution of **2** (30 mg, 0.047 mmol) in ether/CH_3CN (30:1, 10 mL), precooled to 0 °C. Yellow solids slowly precipitated out of the solution. The suspension was filtered after 1 h to give yellow solids of [**2a**]CF_3SO_3 (25 mg, 83% yield). Single crystals of X-ray diffraction quality were obtained from a THF solution with ether diffusion after 10 days at −30 °C.

Data for [2a]CF_3SO_3. ^1H NMR (CD_3CN): δ 1.67 and 2.27 (each s, 3 H, Me), 2.13−2.26 and 2.35−2.49 (each m, 1 H, $IndH(CH_2)_2PPh_2$), 2.84 and 3.19 (each unresolved d, 1 H, $IndH(CH_2)_2PPh_2$), 2.74−2.80 (m, 2 H, H^d and H^f), 3.03−3.15 (m, 2 H, H^b and H^j), 3.28 (s, 2 H, H^{2-3}), 3.51−3.73 (m, 2 H, H^e and H^g), 4.28 and 4.40 (each d, $J = 9.1$ Hz, 1 H, H^a and H^i), 4.92−4.95 (d-liked, 1 H, H^c or H^h), 5.32−5.36 (unresolved td, 1 H, H^c or H^h), 6.26 (s, 1 H, H^1), 6.89−6.92, 7.13−7.21, 7.42−7.44, 7.53−7.61, 7.75−7.81, and 7.98−8.04 (each m, total 14 H, Ph and H^{4-7}). $^{31}P\{^1H\}$ NMR (CD_3-

(24) Alvarez, P.; Lastra, E.; Gimeno, J.; Braña, P.; Sordo, J. A.; Gomez, J.; Falvello, L. R.; Bassetti, M. *Organometallics* **2004**, *23*, 2956.

(25) Pavia, D. L., Lampman, G. M., Kriz, G. S., Eds. *Introduction to Spectroscopy*; Saunders College Publishing, 1996; p 189.

Chart 1. Hydrogen Atom Labeling of the Bis(allyl) and Coordinated LH Ligands

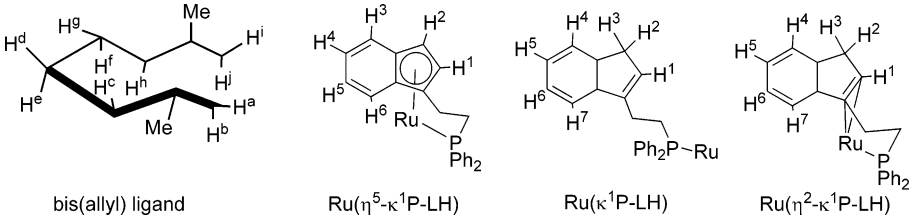

CN): δ 22.2 (s, IndH(CH$_2$)$_2$*P*Ph$_2$). IR (ν cm^{-1}, KBr): 3061 w, 2976 w, 2925 w, 2865 w, 2293 w (CN), 1437 m (CF_3SO_3), 1387 w (CF_3SO_3), 1265 vs (CF_3SO_3), 1223 m, 1151 s (CF_3SO_3), 1032 s (CF_3SO_3), 772 m, 753 m, 699 m, 638 s, 516 m. FAB$^+$-MS: *m*/*z* 601 [M − CH_3CN]$^+$, 565 [M − CH_3CN − Cl]$^+$, 429 [M − CH_3CN − Cl − $C_{10}H_{16}$]$^+$. Anal. Calc (Found) for $C_{36}H_{40}ClF_3NO_3PSRu$: C, 54.6 (54.6); H, 5.1 (5.2); N, 1.8 (1.7).

Synthesis of [(η^5,κ^1*P*-L)Ru(COD)]PF$_6$, [3]PF$_6$. Method 1. COD (6 μL, 0.063 mmol) was injected into a stirred suspension of **2** (30 mg, 0.047 mmol) and $AgPF_6$ (24 mg, 0.095 mmol) in EtOH (10 mL). After 2 h at RT, the suspension was filtered through Celite, giving a yellow filtrate. This was evacuated to dryness and the residue was crystallized from THF/hexane, giving orange-yellow microcrystals of [(η^5,κ^1*P*-**L**)Ru(COD)]PF$_6$, [**3**]PF$_6$ (27 mg, 84% yield).

Method 2. A yellow suspension of **2** (10 mg, 0.016 mmol), Na_2CO_3 (2 mg, 0.019 mmol), KPF_6 (3 mg, 0.016 mmol), and COD (2 μL, 0.021 mmol) in EtOH (5 mL) was refluxed for 4 h. The yellow solids of **2** slowly dissolved upon heating. The solution was evacuated to dryness and extracted using THF. The extract was concentrated to ca. 1 mL, and hexane (ca. 3 mL) was added. Orange-yellow microcrystals of [**3**]PF$_6$ were obtained after 1 day at −30 °C (8 mg, 75% yield). Single crystals of X-ray diffraction quality were obtained from a CH_2Cl_2 solution layered with hexane after 3 days at −30 °C.

Data for [3]PF$_6$. ^{1}H NMR ((CD$_3$)$_2$CO): δ 0.66−0.77 (m, 1 H, COD), 1.28−1.45 (m, 2 H, COD), 1.83−1.98 (m, 2 H, COD), 2.13−2.20 (m, 2 H, COD), 2.32−2.54 (m, 2 H, Ind(C*H*$_2$)$_2$PPh$_2$), 2.60−2.89 (m, 2 H, Ind(C*H*$_2$)$_2$PPh$_2$), 3.52−3.62 (m, 1 H, COD), 3.74−4.04 (m, 4 H, COD), 5.01 (d, $^3J_{HH}$ = 2.5 Hz, 1 H, H^2), 5.12 (br m, 1 H, H^1), 6.70 (t, 1 H, H$^{3-6}$), 7.00−7.03, 7.19−7.24, 7.42−7.48, 7.56−7.71, and 7.75−7.86 (each m, total 13 H, Ph and H$^{3-6}$). ^{31}P{^{1}H} NMR ((CD$_3$)$_2$CO): δ 67.7 (s, Ind(CH$_2$)$_2$*P*Ph$_2$), −142.6 (septet, PF_6). IR (ν cm^{-1}, KBr): 2922 w, 2850w, 1438 w, 1169 w, 1096 w, 836 vs (PF_6), 751 m, 704 m, 557 m (PF_6). FAB$^+$-MS: *m*/*z* 537 [M]$^+$, 429 [M − COD]$^+$. Anal. Calc (Found) for $C_{31}H_{32}F_6P_2Ru$: C, 54.6 (54.7), H, 4.7 (4.8).

Synthesis of [(η^5,κ^1*P*-L)Ru(PPh$_3$)Cl] (4). Method 1. A yellow suspension of **2** (30 mg, 0.047 mmol), Na_2CO_3 (5 mg, 0.047 mmol), and PPh_3 (13 mg, 0.049 mmol) in EtOH (10 mL) was refluxed. The mixture changed to a dark brown homogeneous solution. After heating for 4 h, the solvent was removed under vacuum, and the residue was extracted with toluene (2 × 2 mL). The extract was concentrated to ca. 2 mL and then loaded onto a silica gel column (2 × 5 cm) prepared in *n*-hexane. Elution gave two fractions: (i) a yellow eluate in toluene (6−8 mL), which yielded [(η^5,κ^1*P*-**L**)-Ru(PPh$_3$)H], **5** (5 mg, 15% yield; see synthesis below); (ii) a dark brown eluate in toluene/ether (1:1, 12−15 mL), which yielded dark brown crystals of **4** (20 mg, 58% yield) suitable for X-ray diffraction analysis, upon recrystallization from ether.

Method 2. A procedure similar to method 1 was adopted using 0.5 equiv of Na_2CO_3 (2.5 mg, 0.023 mmol). Dark brown crystals of **4** were obtained in 82% yield (28 mg), while **5** was not formed.

Data for 4. ^{1}H NMR (C_6D_6): δ 1.42−1.52 and 1.52−1.64 (each m, 0.5 H, Ind(C*H*$_2$)$_2$PPh$_2$), 1.89−2.06 (m, 1 H, Ind(C*H*$_2$)$_2$PPh$_2$), 2.26 (s, 1 H, H^1), 2.78−2.91 and 3.10−3.22 (each m, 1 H, Ind-(C*H*$_2$)$_2$PPh$_2$), 4.87 (s, 1 H, H^2), 6.64−6.69, 6.79−6.83, 6.93−7.12, 7.25−7.28, 7.37−7.42, 7.68−7.72, and 8.02−8.07 (each m, total 29 H, Ph and H$^{3-6}$). ^{31}P{^{1}H} NMR (C_6D_6): δ 49.0 and 52.5 (each d, *J* = 26.7 Hz, *P*Ph$_3$, Ind(CH$_2$)$_2$*P*Ph$_2$). FAB$^+$-MS: *m*/*z* 726 [M]$^+$, 691 [M − Cl]$^+$, 464 [M − PPh_3]$^+$, 427 [M − Cl − PPh_3]$^+$. Anal. Calc (Found) for $C_{41}H_{35}ClP_2Ru$: C, 67.8 (67.6); H, 4.9 (5.2)

Synthesis of [(η^5,κ^1*P*-L)Ru(PPh$_3$)H] (5). A brown mixture of **4** (10 mg, 13.8 mmol) and NaOMe (freshly generated from Na (2 mg, 87 mmol) in MeOH (5 mL)) in MeOH/THF (1:1, 10 mL) was refluxed for 2 h. The color of the mixture slowly changed from brownish-yellow to bright yellow. The solvent was evacuated to dryness and the residue extracted with hexane (2 × 4 mL). The hexane extract was concentrated to ca. 1 mL. Yellow solids of **5** (5 mg, 53% yield) were collected after 1 day at −30 °C.

Data for 5. ^{1}H NMR (C_6D_6): δ −13.9 (dd, 1 H, *J* = 23.7, 40.3 Hz, Ru−H), 1.72−1.89 (m, 1 H, Ind(C*H*$_2$)$_2$PPh$_2$), 2.31−2.40 and 2.46−2.53 (each m, 0.5 H, Ind(C*H*$_2$)$_2$PPh$_2$), 3.07−3.18, 3.57−3.69 (each m, 1 H, Ind(C*H*$_2$)$_2$PPh$_2$), 4.78 and 5.48 (each s, 1 H, H^1 and H^2), 6.40−6.43, 6.68−6.73, 6.76−6.84, 6.86−6.94, 7.01−7.08, 7.11−7.14, 7.51−7.54, and 7.91−7.97 (each m, total 29 H, Ph and H$^{3-6}$), and δ 0.39 (s, H_2O). ^{31}P{^{1}H} NMR (C_6D_6): δ 66.1 and 78.8 (each d, *J* = 23.7 Hz, *P*Ph$_3$, Ind(CH$_2$)$_2$*P*Ph$_2$). FAB$^+$-MS: *m*/*z* 691 [M − H]$^+$, 429 [M − PPh_3]$^+$. Anal. Calc (Found) for $C_{41}H_{36}P_2Ru\cdot 1.5H_2O$: C, 68.5 (68.8), H, 5.5 (5.7).

Synthesis of [(η^5,κ^1*P*-L)Ru(2,2′-bipyridyl)]PF$_6$, [6]PF$_6$, and [(κ^1*P*-LH)Ru(2,2′-bipyridyl)Cl]PF$_6$, [7]PF$_6$. A yellow suspension of **2** (30 mg, 0.047 mmol), 2,2′-bipyridyl (8 mg, 0.051 mmol), Na_2CO_3 (5 mg, 0.047 mmol), and KPF_6 (9 mg, 0.049 mmol) in EtOH (10 mL) was refluxed. A red mixture resulted after 4 h. The solvent was removed under vacuum and the residue extracted using THF (2 × 5 mL). The extract was concentrated to ca. 2 mL and loaded onto a neutral alumina (activity III) column prepared in THF. Elution gave four fractions: (i) a yellow eluate in THF (2 mL); (ii) a red eluate in THF/acetone (4:1, ca. 25 mL), which gave [**6**]-PF$_6$ as a red oil (20 mg, 58% yield); (iii) a red eluate in THF/acetone (1:1, ca. 8 mL), which gave [**7**]PF$_6$ (11 mg, 25% yield) as red solids upon recrystallization from CH_2Cl_2/ether (1:10); (iv) a red eluate in MeOH (ca. 1 mL), which gave a trace of an unknown species.

A similar reaction was repeated, using Li_2CO_3 (3.5 mg, 0.047 mmol) instead of Na_2CO_3. The ^{31}P NMR spectrum of the reaction mixture showed the presence of the cationic species [**6**]PF$_6$, [**7**]-PF$_6$, and [**8**]PF$_6$, in the ratio of 1:2:2. Separation of these complexes via silica gel chromatography was futile, as complexes [**7**]PF$_6$ and [**8**]PF$_6$ have similar polarity.

HCl (0.35 mL of 0.1 M) was added into a red solution of [**6**]PF$_6$ (5 mg, 0.007 mmol), and 2,2′-bipyridyl (1.6 mg, 0.01 mmol) in EtOH (0.5 mL) was reluxed for 2 h. The solvent was evacuated to dryness and the residue redissolved in *d*-acetone. ^{1}H and ^{31}P NMR spectroscopy showed the total conversion to [**7**]PF$_6$ and [**8**]PF$_6$ in 2:1 ratio.

A red suspension of [**8**]PF$_6$ (4 mg, 0.003 mmol), 2,2′-bipyridyl (0.4 mg, 0.003 mmol), and KPF_6 (0.5 mg, 0.003 mmol) in EtOH (0.5 mL) was refluxed for 2 h. The resultant red solution was evacuated to dryness and redissolved in *d*-acetone. ^{1}H and ^{31}P NMR spectroscopy showed the total conversion of species **8** to **7**.

Data for [6]PF$_6$. ^{1}H NMR ((CD$_3$)$_2$CO): δ 2.82−3.24 (m, 2 H, Ind(C*H*$_2$)$_2$PPh$_2$), 3.74−3.94 (m, 2 H, (Ind(C*H*$_2$)$_2$PPh$_2$), 5.21 (d, $^3J_{HH}$

Table 2. Crystal and Structure Refinement Data

	2	[**2a**]CF_3SO_3	**3**	**4**	**9**
formula	$C_{33.50}H_{38.25}Cl_2O_{0.13}PRu$	$C_{36}H_{40}ClF_3NO_3PRuS$	$C_{32}H_{34}Cl_2F_6P_2Ru$	$C_{42}H_{37.50}ClO_{0.25}P_2Ru$	$C_{33}H_{35}O_4PRu$
molecular weight	645.83	791.24	766.50	744.68	627.65
space group (cryst syst)	$P\bar{1}$	$P2_1/n$	$P\bar{1}$	$P\bar{1}$	$P2_1/c$
cryst syst	triclinic	monoclinic	triclinic	triclinic	monoclinic
unit cell dimens					
a (Å)	12.1186(4)	14.6702(8)	9.1518(5)	11.1768(12)	29.3586(12)
b (Å)	12.4772(5)	9.0353(5)	13.3458(8)	16.1725(17)	11.4964(4)
c (Å)	20.6703(8)	26.8742(15)	13.6837(8)	21.521(2)	17.9306(7)
α (deg)	90.5620(10)	90	69.821(2)	84.424(3)	90
β (deg)	101.7530(10)	99.9560(10)	75.8110(10)	81.268(3)	106.0200(10)
γ (deg)	96.6540(10)	90	81.523(2)	70.180(3)	90
cell volume (Å ^{3})	3037.5	3508.5(3)	1517.23(15)	3612.8(7)	5816.9(4)
Z	4	4	2	4	8
D_{calc} (g cm^{-3})	1.412	1.498	1.678	1.369	1.433
absorp coeff (mm^{-1})	0.766	0.681	0.859	0.626	0.630
F(000) electrons	1333	1624	776	1530	2592
cryst size (mm^3)	0.28 × 0.16 × 0.14	0.60 × 0.20 × 0.14	0.14 × 0.10 × 0.04	0.10 × 0.06 × 0.02	0.30 × 0.20 × 0.16
θ range for data collection (deg)	2.01 to 29.09	1.48 to 25.00	1.62 to 25.00	0.96 to 25.00	0.72 to 27.50
index ranges	$-16 \le h \le 15$	$-17 \le h \le 16$	$-10 \le h \le 10$	$-13 \le h \le 13$	$-28 \le h \le 38$
	$-16 \le k \le 16$	$-9 \le k \le 10$	$-15 \le k \le 10$	$-19 \le k \le 19$	$-14 \le k \le 14$
	$0 \le l \le 28$	$-31 \le l \le 31$	$-16 \le l \le 13$	$-25 \le l \le 25$	$-23 \le l \le 18$
no. of reflns collected	40 877	19 971	9007	38 904	40 443
no. of indep reflns	14 685	6200	5337	12 708	13 340
max. and min. transmn	0.9003−0.8140	0.9107−0.6855	0.9665−0.8892	0.9876−0.9401	0.9059−0.8335
no. of data/restraints/params	14 685/0/692	6200/42/420	5337/0/388	12 708/58/855	13 340/0/719
GoF	1.101	1.024	1.144	1.185	1.064
final R indices [$I > 2\sigma(I)$]	R1 = 0.0608	R1 = 0.0672	R1 = 0.0713	R1 = 0.1359	R1 = 0.0425
	wR2 = 0.1346	wR2 = 0.1708	wR2 = 0.1453	wR2 = 0.3149	wR2 = 0.0938
R indices (all data)	R1 = 0.0834	R1 = 0.1033	R1 = 0.0898	R1 = 0.1596	R1 = 0.0547
	wR2 = 0.1447	wR2 = 0.1904	wR2 = 0.1537	wR2 = 0.3259	wR2 = 0.1021
largest diff peak and hole (e Å $^{-3}$)	1.122 and −0.801	1.071 and −0.524	1.174 and −0.963	2.991 and −1.541	0.919 and −0.356

= 2.5 Hz, 1 H, H^2), 5.53 (m, 1 H, H^1), 6.82−6.94, 7.07−7.38, 7.44−7.49, 7.54−7.70, 7.80−7.91, 8.35−8.40, and 9.04−9.06 (each m, total 22 H, bipyridyl, Ph and H$^{3-6}$), and δ 1.80 and 3.62 (each m, THF). $^{31}P\{^1H\}$ NMR ($(CD_3)_2CO$): δ 61.7 (s, Ind$(CH_2)_2PPh_2$), −142.6 (septet, PF_6). IR (ν cm^{-1}, KBr): 3054 w, 2923 w, 1436 w, 1265 w, 1161 w, 1096 w, 1029 w, 841 vs (PF_6), 745 w, 699 w, 558 w (PF_6), 518 w. FAB$^+$-MS: m/z 585 [M]$^+$, 429 [M − bipyridyl]$^+$. Anal. Calc (Found) for $C_{33}H_{29}F_6N_2P_2Ru\cdot C_4H_8O$: C, 55.3 (55.3); H, 4.6 (4.1); N, 3.5 (3.4).

Data for [7]PF_6. ^{1}H NMR ($(CD_3)_2CO$): δ 2.25−2.38 (m, 2 H, IndH(CH_2)$_2$PPh$_2$), 2.84−2.91 (m, 2 H, IndH(CH_2)$_2$PPh$_2$), 3.23−3.24 (m, 2 H, H$^{2-3}$), 6.10 (s, 1 H, H^1), 6.91−6.94, 6.96−7.01, 7.03−7.16, 7.24−7.28, 7.38−7.47, 7.52−7.57, 7.63−7.68, 7.78−7.83, 8.00−8.18, 8.23−8.29, 8.48−8.50, 8.64−8.70, 9.17−9.19, and 9.84−9.86 (each m, total 30 H, bipyridyl, Ph and H$^{4-7}$). $^{31}P\{^1H\}$ NMR ($(CD_3)_2CO$): δ 39.5 (s, IndH$(CH_2)_2PPh_2$), −142.6 (septet, PF_6). IR (ν cm^{-1}, KBr): 3069 w, 2921 w, 1459 w, 1439 w, 1162 w, 1096 w, 1025 w, 842 vs (PF_6), 763 m, 558 w (PF_6), 521 w. FAB$^+$-MS: m/z 777 [M]$^+$, 449 [M − (**LH**)]$^+$. Anal. Calc (Found) for $C_{43}H_{36}ClF_6N_2P_2Ru\cdot 1/2CH_2Cl_2$: C, 54.1 (54.2); H, 3.9 (4.2); N, 5.8 (6.2).

Synthesis of { [(κ^1*P*-LH)Ru(2,2′-bipyridyl)]$_2$(μ-Cl$_3$)}PF_6, [8]-PF_6. HCl (0.7 mL of 0.1 M) was added into a red solution of [**6**]-PF_6 (10 mg, 0.014 mmol) in EtOH, and the solution was stirred at RT for 4 h. The resultant red solution was evacuated to dryness. The residue was dissolved in acetone and the solution passed through a short neutral alumina (activity III) column. Subsequent workup of the red eluate in acetone/ether (3:1) gave [**8**]PF_6 as crystalline red flakes (7 mg, 70% yield).

Data for [8]PF_6. ^{1}H NMR ($(CD_3)_2CO$): δ 2.48 (br s, 2 H, IndH-(CH_2)$_2$PPh$_2$), 2.70−2.80 (m, 2 H, IndH(CH_2)$_2$PPh$_2$), 3.23 (s, 2 H, H$^{2-3}$), 6.10 (s, 1 H, H^1), 6.94−6.96, 6.99−7.04, and 7.76−7.81 (each td-like m, 1 H, bipyridyl), 7.13−7.35 and 7.38−7.44 (each m, total 14 H, Ph and H$^{4-7}$), 8.18−8.24 (t-like m, 2 H, bipyridyl), 9.08 and 9.18 (each d, $^3J_{HH}$ = 4.9 Hz, 1 H, bipyridyl). $^{31}P\{^1H\}$ NMR ($(CD_3)_2CO$): δ 54.5 (s, IndH$(CH_2)_2PPh_2$), −142.6 (septet, PF_6). FAB$^+$-MS: m/z 1279 [M]$^+$, 777 [M − Ru(**LH**)Cl$_2$]$^+$, 585 [M − Ru(**LH**)($N_2C_{10}H_8$)Cl$_2$]$^+$, 465 [M − (**LH**)$_2$($N_2C_{10}H_8$)]$^+$, 429 [M − (**LH**)$_2$($N_2C_{10}H_8$)Cl]$^+$. HR-FAB$^+$-MS for $C_{66}H_{56}N_4Cl_3P_2Ru_2$ [M]$^+$: m/z 1278.1131 (found), 1278.1121 (calc). Anal. Calc (Found) for $C_{66}H_{56}Cl_3F_6N_4P_3Ru_2$: C, 55.8 (55.4); H, 4.0 (3.9); N, 3.9 (4.0).

Synthesis of [(η^2,κ^1*P*-L)Ru(acac)$_2$] (9). A yellow suspension of **2** (30 mg, 0.047 mmol), Na_2CO_3 (13 mg, 0.12 mmol), and acetyl acetone (12 μL, 0.12 mmol) in EtOH (10 mL) was refluxed. As the reaction proceeded, a yellow mixture resulted. After refluxing for 4 h, the solvent was removed under vacuum and the residue extracted using hexane (2 × 5 mL). The extract was concentrated to ca. 2 mL and loaded onto a silica gel column (1 × 8 cm) prepared in *n*-hexane. Elution gave two fractions: (i) a yellow eluate in hexane/ether (6:1, 2 mL), which yielded <1 mg of a solid material, probably also of **9**; (ii) a yellow eluate in hexane/ether (4:1, 8 mL), which upon recrystallization from hexane yielded yellow crystals of **9** (23 mg, 78% yield). X-ray diffraction-quality crystals were obtained from a concentrated hexane solution in an NMR tube after 1 h at room temperature.

Data for 9. ^{1}H NMR (CD_2Cl_2): δ 1.34 (s, 3 H, Me), 1.43 (s, 3 H, Me), 1.68 (s, 3 H, Me), 1.80 (s, 3 H, Me), 2.32 − 2.45 (m, 1 H, Ind(CH_2)$_2$PPh$_2$), 2.50−2.73 (m, 2 H, Ind(CH_2)$_2$PPh$_2$), 2.71−2.74 and 2.81−2.89 (each m, 0.5 H, Ind(CH_2)$_2$PPh$_2$), 3.39 (dd, J = 3.7, 20 Hz, 1 H, H^2), 3.61 (d, J = 20 Hz, 1 H, H^3), 4.29 and 4.96 (each s, 1 H, [$(CH_3)C(O)]_2CH$), 5.15 (d, J = 3.7 Hz, H^1), 6.91−6.97, 6.98−7.07, 7.09−7.22, 7.24−7.30, 7.34−7.45, and 7.96−8.03 (each m, total 14 H, H$^{4-7}$), and δ 0.89 and 1.23 (each m, hexane). $^{31}P\{^1H\}$ NMR (CD_2Cl_2): δ 70.4 (s, Ind$(CH_2)_2PPh_2$). IR (ν cm^{-1},

KBr): 3054 w, 2915 w, 2872 w, 2835 w, 1581 s (CO), 1513 vs (CO), 1435 m, 1395 s, 1261 w, 1196 w, 1097 w, 1019 w, 938 w, 855 w, 741 w, 698 m, 603 w, 528 m. FAB$^+$-MS: *m*/*z* 628 $[M]^+$, 528 $[M - acac]^+$, 429 $[M - 2\ acac]^+$. Anal. Calc (Found) for $C_{33}H_{35}O_4PRu \cdot 1/4C_6H_{12}$: C, 63.8 (63.8); H, 5.9 (5.6).

Crystal Structure Determinations. Crystals were mounted on quartz fibers. X-ray data were collected on a Bruker AXS APEX system, using Mo Kα radiation, with the SMART suite of programs.[26] Data were processed and corrected for Lorentz and polarization effects with SAINT[27] and for absorption effects with SADABS.[28] Structural solution and refinement were carried out with the SHELXTL suite of programs.[29] Crystal and structure refinement data are summarized in Table 2. The structures were solved by direct methods or Patterson maps to locate the heavy atoms, followed by difference maps for the light, non-hydrogen atoms. All non-hydrogen atoms were generally given anisotropic displacement parameters in the final model.

The crystal of **2** contained a diethyl ether solvent molecule with partial occupancy. This was modeled as disordered over an inversion center.

(26) *SMART* version 5.628; Bruker AXS Inc.: Madison, WI, 2001.
(27) *SAINT*+ version 6.22a; Bruker AXS Inc.: Madison, WI, 2001.
(28) Sheldrick, G. M. *SADABS*, 1996.
(29) *SHELXTL* version 5.1; Bruker AXS Inc.: Madison, WI, 1997.

Acknowledgment. The authors acknowledge with thanks support from the Academic Research Fund (grant no. 143-000-209-112 to L.Y.G.) and Institute of Chemical and Engineering Sciences for a research scholarship to S.Y.N.

Supporting Information Available: Complete crystallographic data in CIF format for **2**, **2a**, **3**, **4**, and **9** and ^{1}H NMR (500 MHz) spectrum of **9** showing signals of H^{1-3}. This material is available free of charge via the Internet at http://pubs.acs.org.

OM070225J